JOURNAL OF PROPULSION AND POWER
Vol. 11, No. 6, November–December 1995

Feedback-Controlled Gas Mixing System for the Ram Accelerator

M. R. Jardin* and A. P. Bruckner†
University of Washington, Seattle, Washington 98195

A feedback-controlled gas mixing system is presented along with operational results for a prototype implementation, which has been developed for the University of Washington ram accelerator hypervelocity launcher facility. The control system is designed to fill high-pressure chambers with a selected number of component gases (four for the ram accelerator) at a chosen set of molar ratios. A mass flow rate controller keeps the mass flow rate of a primary gas constant while secondary gas controllers drive the molar ratio errors to zero, thereby ensuring that the final gas composition is correct. The sensing elements are resistive thermal detection mass flow meters and the control elements are switched servoactuated metering valves. Experimental results for the operation of the prototype system are reported.

Nomenclature

A = area
C_v = valve C_v factor, a measure of pressure loss in gallons per minute of water that will pass through an orifice with a pressure differential of 1 psi
c_p = specific heat at constant pressure
D = diameter; denominator polynomial of a transfer function
$d_{\min}$ = minimum fill line diameter
E = absolute value of the average of E_m
E_D = discretization error
E_{MR} = percent error in mass ratio
E_m = measurement error in mass flow meter
K_{cf} = conversion constant in mass flow rate equation
K_{cl} = control law gain
K_{cv} = proportional constant between orifice area and C_v factor
K_{eff} = effective closed-loop system gain
K_F = filter gain
K_{fd} = relational constant between C_v factor and molar flow rate
K_{ss} = steady-state gain of the control law
K_v = rate of change of the C_v with respect to time
L = length of fill pipe
M = Mach number
M_a = true accumulated mass
$\dot{M}_{cl}$ = voltage signal from control law in feedback loop
M_e = accumulated mass with error due to discrete integration and measurement error in the mass flow meter
$\dot{M}_e$ = error signal in feedback loop and input to control law
$\dot{M}_{filt}$ = filtered mass flow rate signal
$\dot{M}_m$ = mass flow rate reading from flow meter
$\dot{M}_{max}$ = maximum mass flow rate
$\dot{M}_p$ = mass flow rate of the primary gas
$\dot{M}_{ref}$ = input reference mass flow rate
$\dot{M}_{SLM}$ = mass flow rate in standard liters per minute
$\dot{M}_s$ = mass flow rate of the secondary gas
$\dot{m}$ = mass flow rate in kg/s
N = numerator polynomial of a transfer function
P = pressure; pole of a transfer function
P_s = standard pressure, 1.01×10^5 MPa
P_t = total pressure
R = ideal gas constant for a given gas
Re = Reynolds number
R_u = universal ideal gas constant
$\dot{R}_n$ = angular speed of valve actuator motor shaft, rev/s
$\mathcal{R}$ = molar ratio of two gases
s = complex variable, Laplace transform analysis
T = temperature, absolute
T_s = standard temperature, 273.15 K
T_t = total temperature
u = axial flow velocity
V = volume
V_{DZ} = dead-zone voltage
V_e = error voltage
W = molecular weight
Z = zero of a transfer function
γ = ratio of specific heats
ε = pipe roughness coefficient, in.
ρ = density
Φ = friction coefficient

Subscripts
f = conditions in the fill tank
G = forward path transfer function
H = feedback path transfer function
v = conditions at the valve orifice
1 = conditions upstream of the valve orifice
2 = conditions downstream of the valve orifice

Presented as Paper 94-0016 at the AIAA 32nd Aerospace Sciences Meeting and Exhibit, Reno, NV, Jan. 10–13, 1994; received May 27, 1994; revision received March 7, 1995; accepted for publication March 7, 1995.

*Aerospace Engineer, Aerospace and Energetics Research Program; currently at NASA Ames Research Center, Air Traffic Management Branch, M/S 210-9, Moffett Field, CA 94035. Member AIAA.

†Professor of Aeronautics and Astronautics, Aerospace and Energetics Research Program. Associate Fellow AIAA.

Introduction

THE ram accelerator is a device that accelerates objects to hypersonic velocities by use of a chemical propulsion cycle very similar to that of a conventional ramjet.[1] In the ram accelerator, the projectile is shaped like the centerbody of a ramjet and travels freely through a tube filled with a mixture of combustible gases. The shock structure that is developed as the projectile moves through the gases stabilizes combustion behind the projectile, causing acceleration (Fig. 1).

Recent studies[2] suggest that slight changes in gas composition can have significant effects upon ram accelerator performance so that obtaining accurate gas mixtures is very important. In addition to high accuracy, the system used to fill the ram tubes prior to a projectile launch must be quick and efficient if the ram accelerator is to emerge from the research laboratory and become a practical hypersonics test-bed or orbital launch facility in the future.

Both the sonic orifice method for setting ratios of mass flow rates and partial pressure filling have been used for creating the required combustible gas mixtures, but both methods have inherent problems that have necessitated the search for an alternative gas mixing system. Three requirements must be met in order to improve upon the current systems: 1) direct measurement of mass flow rate or of total mass must be made in real time, 2) all gas components should be allowed to flow simultaneously for more efficient operation, and 3) mass ratios should be measured and should be able to be set to a specified high degree of accuracy. A feedback-control mechanism that makes use of true mass flow meters along with integrating capabilities can meet all of the requirements. The concept is to set the mass flow rate of a primary gas component constant with a mass flow rate controller and then to flow the secondary gases through mass ratio controllers using the mass flow rate of the primary gas as a reference input (Fig. 2).

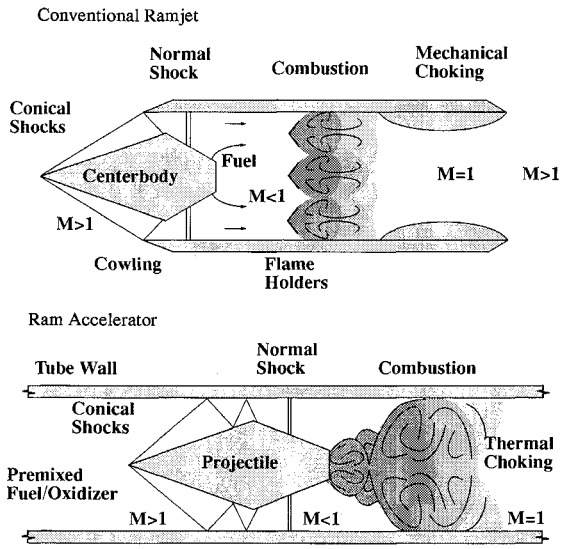

Fig. 1 Ram accelerator operates on a chemical propulsion cycle similar to that of a conventional ramjet.

The organization of this article follows a fairly standard methodology for control system design. The analysis and subsequent selection of control components (mass flow meter, control valve, and actuator) are given first, followed by the dynamic modeling of all elements of the prototype gas mixing system. Once the dynamic modeling has been shown, the mass flow rate control law design is given, followed by the design of the mass ratio control law. Finally, experimental results and conclusions are presented.

Control Component Selection

The resistive thermal detection (RTD) mass flow meter, which accurately measures the true mass flow rate (as opposed to volume flow rate) of a gas via heat transfer principles, best meets the mass flow meter requirements as stated in the Introduction. Measuring mass flow rate instead of volume flow rate eliminates the need for extensive pressure and temperature corrections.[3]

The RTD mass flow meter measures mass flow rates by transferring heat to a diverted stream of the flowing gas and measuring the temperature rise a little further downstream by the use of resistive thermal heating coils in a bridge circuit (Fig. 3). Heat transfer to a flowing gas is primarily dependent upon mass transport and the specific heat of the gas, so that the mass flow rate can be detected by this principle. Since c_p is a weak function of temperature, a very small correction factor is needed for variations in gas temperature ($\pm 0.2\%$ of full-scale flow per degree Celsius between 0–50°C).

A micrometering needle valve is employed as the mass flow control element since these valves can withstand high pressures and can provide desirable flow characteristics over the control system operating range. A servoactuator with a custom designed control board is used for its flexibility in adjusting actuator parameters.

A Macintosh IIci running National Instruments Labview version II software is employed for implementation of the control laws. A National Instruments NB-MIO-16L multifunction analog/digital and timing board provides the hardware/computer interface, and a special termination board, the National Instruments SC-2070, is employed for its thermocouple cold-junction compensation capabilities. Two pressure transducers and two thermocouples are used to make independent measurements of mass vs time in both the source gas tank and the fill tank into which the gases are to be flowed. These probes and transducers consist of one each of a PX603-1KG5V 1000-psig pressure transducer and a PX603-3KG5V 3000-psig pressure transducer and two JTIN-18E-12 J-type thermocouple probes from Omega Engineering, Inc.

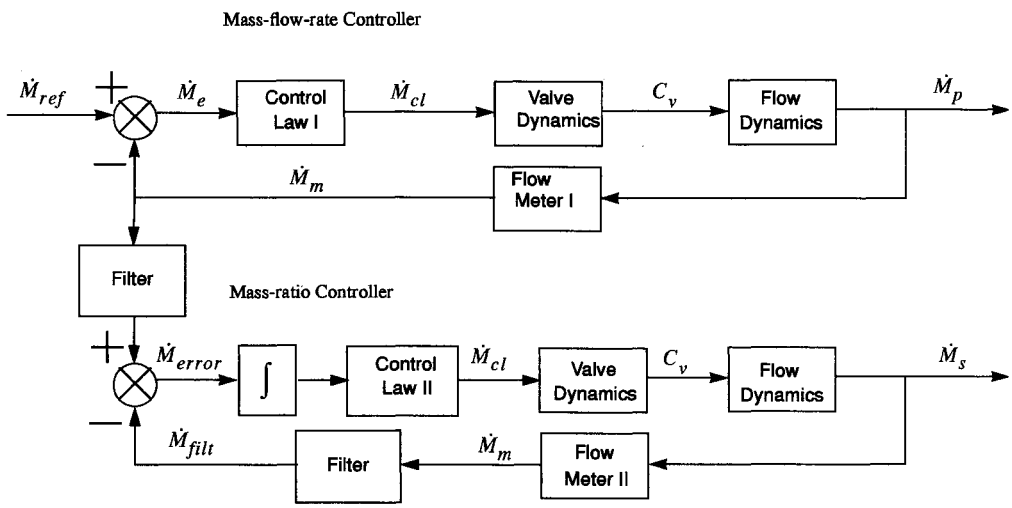

Fig. 2 Mass flow rate of a primary gas is held constant with one control loop and the output is used as a reference command for a separate control loop that maintains a constant mass ratio between two (or more) gases.

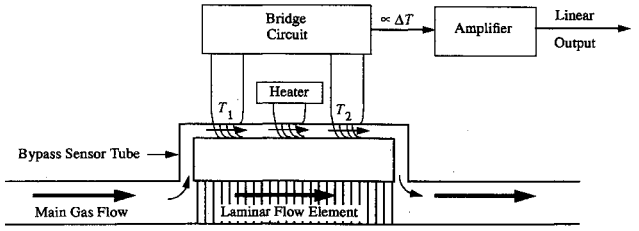

Fig. 3 In the RTD measurement concept, heat is transferred to a flowing gas, and the temperature rise of the gas is measured in a bridge circuit and is proportional to the rate of mass flow.

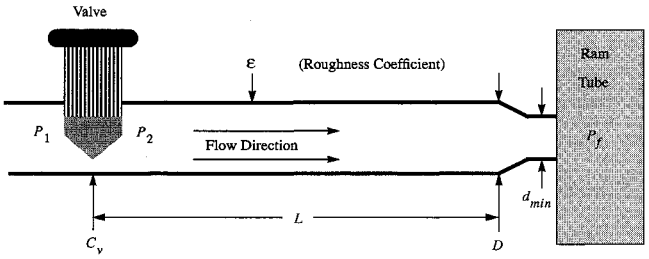

Fig. 4 Gas fill system model used for valve-sizing calculations.

Mass Flow Meter Sizing

When choosing the measurement range of mass flow rates for the mass flow meter, the total mass to be flowed and the total time required for a fill process must be considered. Knowing the volume and pressure to which the gases must be filled allows the total mass to be computed, while the required time is a function of the gasdynamic limits of the fill system hardware, the type of gas, the desired gas mixture, and the desired accuracy of the mass flow meter. After all of the previous factors were considered, a Teledyne–Hastings Raydist (model HFM-201) mass flow meter was selected with a range of 200 standard liters per minute (SLM; the number of liters per minute of a gas flowing at 1 atm and 0°C).

Control Valve and Actuator Sizing

The control valve must be large enough to allow the upper limit mass flow rates, but must also have desirable control characteristics at the lower mass flow rates. The actuator must integrate well with the valve to achieve these goals. The objective of the following calculations is to obtain a numerical algorithm that gives the valve C_v factor (an empirical measure of valve size used by most valve manufacturers[4]) as a function of the measurable and independent parameters in the fill system; namely the mass flow rate $\dot{M}$, upstream total pressure P_{t_1}, ram tube fill pressure P_f, and all of the physical hardware parameters such as tube diameter and the friction coefficient of the tube walls. Once C_v factors have been calculated, the appropriate valve can be chosen. The idealized gas fill system used for these calculations (Fig. 4) has been modeled as a control valve at the beginning of a high L/D fill tube leading into a large plenum (a section of ram tube). One-dimensional, compressible fluid dynamics with friction accounted for will be used to form the necessary relations among the appropriate variables.

Employing the continuity equation along with isentropic relations gives the fairly well-known equation for the mass flow rate of a calorically perfect gas through a channel of varying cross section A_v

$$\dot{m} = A_v \left[\frac{2\gamma}{(\gamma - 1)RT_1}\right]^{1/2} P_1 \left[\left(\frac{P_v}{P_1}\right)^{2/\gamma} - \left(\frac{P_v}{P_1}\right)^{(\gamma+1)/\gamma}\right]^{1/2} \tag{1}$$

Writing the A_v term as a linear function of the C_v factor, adding a conversion factor to express the mass flow rate $\dot{M}_{\mathrm{SLM}}$ in units of SLM, and solving for the C_v factor yields

$$C_v = \dot{M}_{\mathrm{SLM}}\{K_{\mathrm{cf}} \cdot K_{cv} \cdot P_1[(P_v/P_1)^{2/\gamma} - (P_v/P_1)^{(\gamma+1)/\gamma}]^{1/2}\}^{-1} \tag{2}$$

where

$$K_{\mathrm{cf}} = 1315.74 \sqrt{\frac{\gamma}{(W)(\gamma - 1)}} \left(\frac{L}{N \cdot \mathrm{min}}\right) \tag{3}$$

Note that the $1/\sqrt{T_1}$ term from Eq. (1) is included in K_{cf}, where T_1 is assumed to be room temperature (300 K).

From this point, we need to determine P_v as a function of known values. This will be achieved by working backwards from known conditions at the large plenum, taking into account the pressure losses due to friction along the high L/D fill tube.

Following the work by Shames,[5] which addresses pressure loss along the fill pipe due to shear stress at the pipe wall, a relation between the upstream Mach number and other system parameters is given as

$$\left(\frac{1}{M_2} - \frac{1}{M_f}\right) + \left(\frac{\gamma + 1}{2}\right) \times \ln\left\{\frac{M_2^2[2 + (\gamma - 1)M_f^2]}{M_f^2[2 + (\gamma - 1)M_2^2]}\right\} = \frac{\Phi\gamma}{D} L \tag{4}$$

where M_2 and M_f are the Mach numbers at upstream station 2 and at the entrance to the ram tube just prior to the fitting restriction, respectively. The constant diameter of the fill pipe is given by D and L is the length of the fill pipe. The friction coefficient Φ is a function of the Reynolds number, the diameter of the fill pipe, and the pipe roughness parameter ε, and for the Reynolds numbers of interest can be written as

$$\Phi = \frac{0.25}{\{\log(\varepsilon/3.7 \cdot D) + [5.74/(Re)^{0.9}]\}^2} \tag{5}$$

where the parameters ε and D have been empirically determined for the ram accelerator fill pipe to be 0.03175 and 3.861 mm, respectively.

Employing the continuity equation, the ideal gas law, the definition of the Mach number, and adding a unit conversion factor, an expression for the Mach number at the entrance to the ram tube can be derived as

$$M_f^2 = \left[\frac{\dot{M}_{\mathrm{SLM}} P_s}{P_f A_f (6 \times 10^4)}\right]^2 \frac{W}{\gamma T_f R_u} \tag{6}$$

where all of the variables must be expressed in SI units, except $\dot{M}_{\mathrm{SLM}}$, which is in SLM.

Isentropic relations along with the continuity equation, the definition of the Mach number and the ideal equation of state give

$$P_2 = \frac{\dot{m}}{A_2 M_2} \left(\frac{R \cdot T_{t_2}}{\gamma\{1 + [(\gamma - 1)/2]M_2^2\}}\right)^{1/2} \tag{7}$$

Finally, by assuming isentropic, incompressible conditions from the exit plane of the valve to station 2 and employing the continuity equation and Euler's equation, the pressure at the valve orifice is shown to be

$$P_v = P_2 \left\{\frac{\gamma M_2^2}{2}\left[1 - \left(\frac{A_2}{C_v \cdot K_{cv}}\right)^2\right] + 1\right\} \tag{8}$$

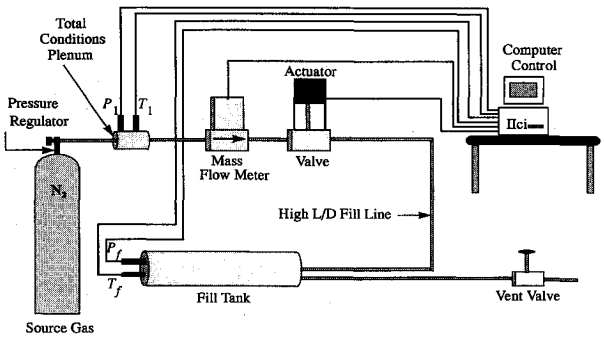

Fig. 5 Prototype control system schematic.

Equations (2–8) constitute a complete set of relations that may be iteratively solved for the required valve C_v factor as a function of known system parameters and flow conditions. These equations have been numerically solved for the range of flow conditions that the control system must cope with, and, along with considerations of linearity and fine-control capability, have helped to determine that the Whitey SS-21RS4 micrometering valve ($0 \leq C_v \leq 0.007$) will integrate well with the control system.

The actuation of the valve has been achieved with a switched servomotor provided by ETI Systems. The standard motor speed of 8 rpm yields a 3 SLM/s rate of change in the mass flow rate under typical controller operating conditions that provides fine control capability without sacrificing speed of operation.

Prototype Dynamic Modeling

Referring to Fig. 5, the mass flow meter has been placed immediately upstream of the control valve. In this way the meter and valve can be kept close together, but any turbulence added to the flow by the valve will not affect the meter. Additionally, having the meter upstream of the valve keeps the pressure of the gas flowing through the meter roughly constant, which increases the precision of the mass flow measurements.

Mass Flow Meter Dynamic Response Measurements

The time response of the mass flow meter can be accurately modeled as a simple first-order lag. Step changes in mass flow rate were applied to the mass flow meter by quickly opening or closing a valve and recording the meter output voltage. The response data were normalized to a final value of unity and the resulting transfer function for the flow meter has been determined to be

$$\frac{\dot{M}_m(s)}{\dot{M}(s)} = \frac{5.85 \times 10^{-3}}{(s + 0.2339)} \frac{\text{V}}{\text{SLM}} \tag{9}$$

with a conversion factor of 0.025 (V/SLM) included since the output of the meter is in volts, and the mass flow rate is treated in SLM (Fig. 6).

Control Valve and Actuator Modeling

The control valve C_v factor is accurately modeled as a linear function of the number of revolutions of the valve stem, and the motor speed of the switched actuator is modeled by a constant value, either positive or negative depending upon the sign of the input voltage. The mathematical model for the valve is the following:

$$\frac{dC_v}{dt} = \pm K_{v_a} \tag{10}$$

Table 1 Valve/actuator parameters

$\dot{R}_n$, rev/s	$\Delta(C_v)/\Delta(R_n)$, gpm_1/rev	K_{v_a}, gpm_1/s
1.261×10^{-1}	9.33×10^{-4}	1.177×10^{-4}

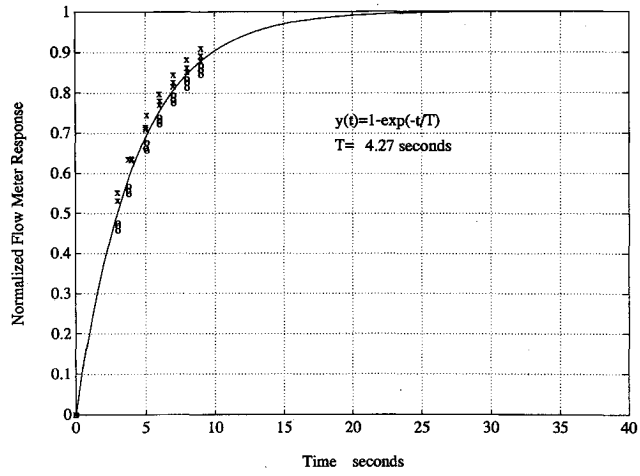

Fig. 6 Measurements of the mass flow meter response to a step input were made for several mass flow rates and the results normalized to unity. The data was then fit with a first-order exponential decay function as shown.

An equation can easily be written for K_{v_a} in terms of measurable quantities in the following way:

$$K_{v_a} = \dot{R}_n[\Delta(C_v)/\Delta(R_n)] \tag{11}$$

where R_n is the number of revolutions of the valve stem. These quantities have been empirically determined and are given in Table 1 along with the value for K_{v_a}, where gpm_1 refers to the units of the C_v factor (gallons per minute of water that will flow through the orifice with a pressure drop of 1 psi).

Due to the actuator motor switch, regardless of the magnitude of the input voltage, the rate at which the motor turns is constant. This simple nonlinearity is easily analyzed in terms of the equivalent describing function linear model, which is a gain term that is a function of the actuator input voltage $\dot{M}_{\text{cl}}$, as shown next:

$$K_v = (4/\pi) \cdot (K_{v_a}/|\dot{M}_{\text{cl}}|) \tag{12}$$

This gives the following linearized transfer function for the C_v factor:

$$C_v(s)/\dot{M}_{\text{cl}}(s) = K_v/s \tag{13}$$

The maximum value of K_v will occur near steady-state conditions when $|\dot{M}_{\text{cl}}(s)|$ is a minimum. The valve actuator contains a dead-zone V_{DZ} between ± 0.02 V so that the value of K_v will never become infinite in the prototype control system and the gain of the compensator will be able to change the error value magnitude at which the system reaches steady state. The maximum value of K_v to be encountered during operation is given approximately by the following relationship:

$$K_{v_{\max}} = \frac{4}{\pi} \cdot \frac{K_{v_a} \cdot K_{\text{cl}} \cdot \prod Z_{\text{cl}}}{|V_{\text{DZ}}| \cdot \prod P_{\text{cl}}} \tag{14}$$

where the subscript cl refers to the elements of a forward-loop control law (Fig. 2). This relationship will be employed

during the control law design phase to help determine stability limits.

Mass Flow Rate Dynamics

A simplified model of the mass flow rate dynamics is obtained by rearranging Eq. (2) to obtain

$$\dot{M}_{\mathrm{SLM}} = K_{\mathrm{cf}} C_v K_{cv} P_1 [(P_v/P_1)^{2/\gamma} - (P_v/P_1)^{(\gamma+1)/\gamma}]^{1/2} \quad (15)$$

K_{cv} is empirically determined by setting the valve to a known C_v factor and by setting P_1 and P_v to known values and then measuring $\dot{M}_{\mathrm{SLM}}$. These measurements lead to the following value:

$$K_{cv} = 7.1475 \times 10^{-5} \quad (16)$$

Making use of Eq. (15) a linearized transfer function for the mass flow rate dynamics is obtained by noticing that the pressure terms will generally remain constant during normal operations of the control system (choked flow and regulated upstream pressure P_1). However, if P_1 should drop below the regulator level, the volume of the source gas plenum is relatively large so that the rate of change of P_1 will be very small compared to the other dynamic terms in the system. If the flow through the control valve should unchoke, since the ram tubes also have large volumes, the P_v/P_1 terms will also have relatively small rates of change. Therefore, the mass flow rate dynamics may be adequately described with the following linear transfer function:

$$\dot{M}_{\mathrm{SLM}}(s) = K_{fd} \cdot C_v(s) \quad (17)$$

where K_{fd} will have a range of values for which the control laws must be designed to operate.

The upper gain limit, easily determined by the use of Eq. (15), occurs when the flow through the valve is choked and the upstream pressure is at the maximum value of 1000 psig. The minimum gain is slightly more difficult to find, but can be computed with the help of the computer program that was used for sizing the control valve. By running the program for the case where P_f is a minimum (about 400 psig for the ram accelerator) and where the mass flow rate is a minimum (about 50 SLM for nitrogen), the computed values of P_1 and P_v corresponding to the maximum C_v factor for the valve (0.007) can be used to determine the maximum gain [Eq. (18)]:

$$7 \times 10^3 \leq K_{fd} \leq 60 \times 10^3 \quad (18)$$

These limits define the gain range for which the gas mixing system must provide robust control.

Mass Flow Rate Control Law Design

As mentioned in the Introduction the control of the mass ratio of two (or more) gases is achieved by setting the mass flow rate of a primary gas to a constant value and then controlling the integrated mass ratio of the secondary gas(es) relative to the primary gas with a separate control law.

The block diagram representation of the mass flow rate controller appears in Fig. 7. As noted earlier, the switching action of the valve means that the gain of K_{cl} is unable to adjust system dynamics in the usual way. The control law gain can scale the actuator input voltage such that steady state is reached at a desired level of mass flow rate accuracy, but the actuator will open (or close) the valve at the same rate regardless of the magnitude of the input voltage; the actuator only differentiates between positive and negative voltage. For this reason, the control law dynamic parameters (poles and zeros) must be chosen such that the system response will be robust over the entire variable gain range.

As previously mentioned, the valve actuator has a deadzone between ± 0.02 V so that if the input to the actuator

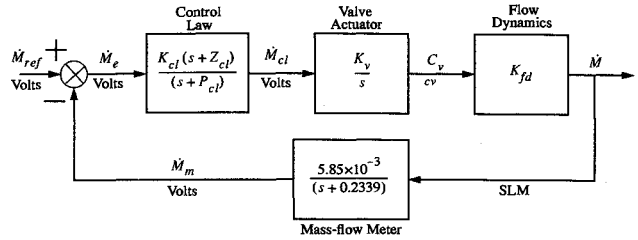

Fig. 7 This block diagram represents the system model used for analyzing the mass flow rate controller.

drops within this range, the control system will be in steady state. This is not desirable until the mass flow rate has been set to an acceptable level of accuracy. K_{cl} can be used to scale the actuator input voltage in order to set the accuracy of the mass flow rate controller, carefully noting that too high of a value for K_{cl} may cause continuous small-amplitude oscillations due to system noise.

An expression for the steady-state error in terms of percent error is given by

$$\dot{M}_e = \dot{M}_{\mathrm{ref}}[1 - (\dot{M}_m/\dot{M}_{\mathrm{ref}})] = \dot{M}_{\mathrm{ref}} E_p \quad (19)$$

where E_p is the percent error between the measured mass flow rate and the reference command mass flow rate.

The steady-state gain of the control law will be given by the following equation:

$$K_{\mathrm{ss}} = K_{\mathrm{cl}} \cdot \prod Z \Big/ \prod P \quad (20)$$

When the steady-state gain is multiplied by the desired minimum steady-state error term, the result should equal 0.02 V or greater so that the valve actuator will still actively control the flow to this point. Multiplying Eqs. (19) and (20) and solving for K_{cl} gives

$$K_{\mathrm{cl}} = \frac{(0.02) \prod P}{\prod Z \cdot \dot{M}_{\mathrm{ref}} \cdot E_p} \quad (21)$$

This equation is easily programmed to allow the user of the control system to set the control law gain for any desired value of E_p.

For a simple first-order control law, the range of effective system gain for which the compensator must provide robust control can be found by applying Eqs. (14) and (18). Utilizing root locus plots and nonlinear simulations quickly helps to determine that the following control law will provide robust control without excessive oscillations to set the mass flow rate to within 1% of the maximum command value (200 SLM, or 5 V):

$$\frac{\dot{M}_{\mathrm{cl}}(s)}{\dot{M}_e(s)} = \frac{17.1(s + 0.2339)}{(s + 10)} \quad (22)$$

Note that the gain margin for the system with this particular control law can easily be shown to be infinite so that stability of the control system is guaranteed for all positive gain values.

Mass Ratio Control Law Design

For mass ratio control, as seen in the block diagram (Fig. 8), an integrator must be added to the control law in order to drive the mass ratio error (not just the error in the ratio of mass flow rates) to zero, and this places a second pole at the origin, bringing the system transfer function to third-order.

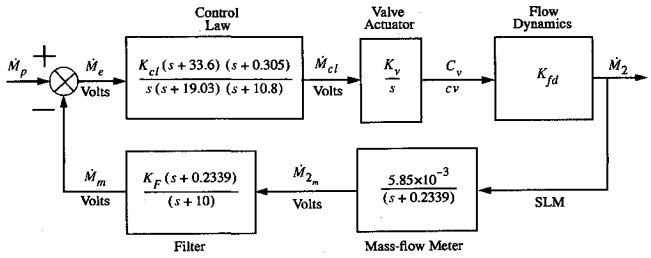

Fig. 8 With the addition of the integrator in the forward loop, and the filter in the feedback path, the control of mass ratios can be achieved.

Since the reference input value $\dot{M}_p$ is the mass flow rate of the primary gas, the feedback value $\dot{M}_{\text{filt}}$ must be made to represent what the mass flow rate of the primary gas should be in order to obtain the correct mass ratio between the secondary and primary gases. Defining the desired mass ratio in the following way:

$$\mathcal{R}_s = (\dot{M}_s/\dot{M}_p)_{\text{desired}} \tag{23}$$

the feedback term must be, simply,

$$\dot{M}_{\text{filt}} = \dot{M}_s/\mathcal{R}_s \tag{24}$$

The desired mass ratio $\mathcal{R}_s$ is known, but $\dot{M}_s$ is not directly available in this system. The measurement of the mass flow rate comes from the mass flow meter that equals the true mass flow rate only in steady state. A filter may be employed, however, which effectively compensates for the lag in the reading from the mass flow meter. This minimizes the integral error so that the mass ratios may be much more quickly set. Without the filter, an overshoot of a few percent with a very long decay time constant must be tolerated, as was discovered during nonlinear simulations and during subsequent testing of the mass ratio control system.

The system transfer function with the mass flow meter pole effectively canceled by the filter is given by

$$\frac{\dot{M}_s}{\dot{M}_p} = \frac{K_{fd}K_vN_{\text{cl}}(s+10)}{[s^2(s+10)D_{\text{cl}} + K_{fd}K_vN_{\text{cl}}K_F(5.85\times10^{-3})]} \tag{25}$$

where N_{cl} and D_{cl} are the numerator and denominator dynamic terms of the control law, and K_F is defined such that the steady-state gain of the filter is equal to $1/\mathcal{R}_s$. The definition is, simply,

$$K_F = \frac{10}{(0.2339)\mathcal{R}_s} \tag{26}$$

The use of a third-order controller (in addition to the integrator) makes the characteristic equation of the closed-loop transfer function sixth-order. The third-order controller has six parameters (three poles and three zeros), which may be used to set the poles of the system transfer function as desired. One must only be careful to adhere to any physical limits imposed by the system hardware.

The denominator polynomial of the system transfer function is written as

$$D_W(s) = D_G(s)\cdot D_H(s)\cdot[(s+P_1)(s+P_2)(s+P_3)] + N_G(s)\cdot N_H(s)\cdot[(s+Z_1)(s+Z_2)(s+Z_3)] \tag{27}$$

When the pole and zero terms are expanded and the constant terms are placed on the right side, Eq. (27) can be written in the following summation form:

$$\sum_{j=1}^{3}\{[D_G(s_n)\cdot D_H(s_n)\cdot s_n^{(3-j)}]\cdot a_{(j-1)} + [N_G(s_n)\cdot N_H(s_n)\cdot s_n^{(3-j)}]\cdot a_{(j+2)}\} = -s_n^3[D_G(s_n)\cdot D_H(s_n) + N_G(s_n)\cdot N_H(s_n)] \tag{28}$$

with

$$a_0 = P_1 + P_2 + P_3 \tag{29}$$

$$a_1 = P_1\cdot P_2 + P_1\cdot P_3 + P_2\cdot P_3 \tag{30}$$

$$a_2 = P_1\cdot P_2\cdot P_3 \tag{31}$$

$$a_3 = Z_1 + Z_2 + Z_3 \tag{32}$$

$$a_4 = Z_1\cdot Z_2 + Z_1\cdot Z_3 + Z_2\cdot Z_3 \tag{33}$$

$$a_5 = Z_1\cdot Z_2\cdot Z_3 \tag{34}$$

Equation (28) must then be written n times ($n = 6$ in this case), once for each value of s_n that coincides with a desired pole location of the system transfer function. The resulting values for a_n must be used in conjunction with Eqs. (29–34) to solve for the control law pole and zero values. The third-order control laws found in this way for this system generally have a pole and a zero at nearly equal values, which can be canceled to reduce the control law order to 2. This simplifies the implementation of the control system and through analysis was shown not to significantly alter the system response.

Through iterative frequency response analysis of the linearized system, and through simulations of the nonlinear system, the following control law design has been shown to produce desirable characteristics:

$$\frac{\dot{M}_{\text{cl}}(s)}{\dot{M}_e(s)} = \frac{K_{\text{cl}}(s+33.6)(s+0.305)}{s(s+19.03)(s+10.8)} \tag{35}$$

and the filter transfer function is given by

$$\frac{\dot{M}_{\text{filt}}}{\dot{M}_{s_m}} = \frac{(42.7533)(s+0.2339)}{\mathcal{R}_s\cdot(s+10)} \tag{36}$$

Once again utilizing Eq. (21), a control law gain of $K_{\text{cl}} = 8.02$ is determined to set the steady-state mass flow rate of the secondary gas to within 1% of the maximum mass flow rate (200 SLM, or 5 V). Analysis of this control law demonstrates that the system is stable for the entire effective gain range of the system [computed with Eqs. (14) and (18)]. As the effective gain approaches zero (as would happen if the error term approached infinity), the gain margin approaches infinity and the phase margin approaches zero. The gain margin monotonically decreases to a value of 2.13 db at the maximum effective system gain ($K_{\text{eff}_{\max}} = 354$). The phase margin increases to a maximum of 61.0091 deg at $K_{\text{eff}} = 35$ and then decreases to a value of 8.11 deg at $K_{\text{eff}_{\max}}$. Note that even if this system is driven to instability (by increasing K_{cl} too much), this will only result in a small amplitude steady-state oscillation. This is due to the manner in which the nonlinear actuator motor switch operates. As the error term increases, the effective system gain decreases, and this brings the effective system gain back into the stable region. Nonlinear simulations have again been used to verify the results of the linear analysis and have also been used to help tune the controller parameters for a desirable output response.

Experimental Results

A Macintosh IIci running Labview II software from National Instruments has been employed for data acquisition and the implementation of the discretized continuous time control laws developed previously. Several data runs have been made with both the mass flow rate controller and the mass ratio controller flowing nitrogen gas in order to demonstrate the following:

1) The mass flow meter is capable of accurately measuring the true mass flow rate of a gas in real time over a wide range of operating conditions.

2) The mass flow rate controller is capable of setting and maintaining constant mass flow rates to within a high degree of accuracy.

3) The mass ratio controller is capable of setting and maintaining the mass ratio between two gases to within a high degree of accuracy.

Mass Flow Rate Controller

With a unity feedback scheme (no control dynamics), the mass flow rate controller is stable, but the step response is oscillatory with a relatively long decay constant (Fig. 9), which shows that a control law is required for mass flow rate control.

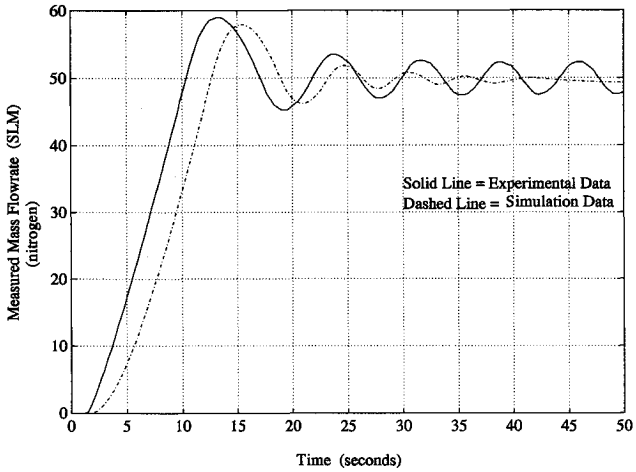

Fig. 9 Response of the mass flow rate control system to a 50 SLM step command with a simple unity feedback scheme showing that control dynamics are necessary. Both experimental and simulation data appear in the plot. Upstream pressure: 1000 psig.

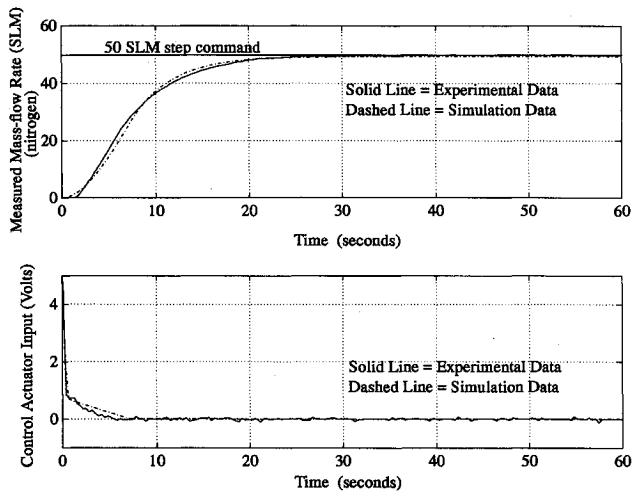

Fig. 10 With the first-order control law in operation, the step response of the mass flow rate controller is greatly improved. Note that the control voltage input to the actuator indicates steady-state conditions have been reached within 6 s, approximately 20 s before the mass flow meter can verify this. Upstream pressure: 1000 psig.

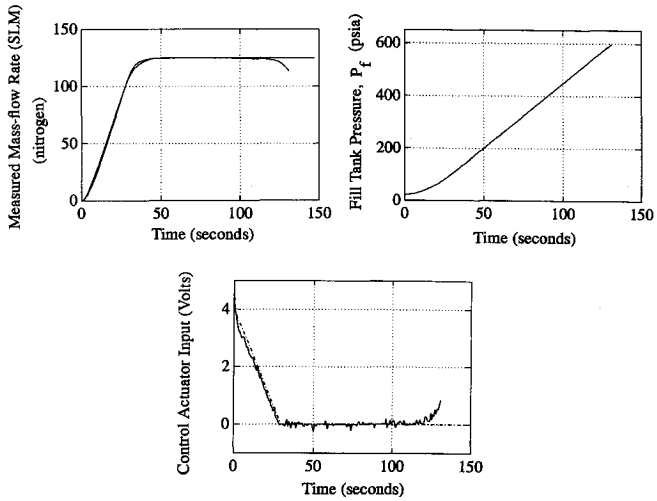

Fig. 11 With a lower upstream pressure of 625 psig, the control system still demonstrates excellent performance. The command mass flow rate is maintained until the fill tank pressure reaches about 85% of the upstream pressure. The theoretical unchoking point occurs at P_f = 305 psia, which corresponds to t = 71 s.

Notice that although the nonlinear simulation data does not match exactly with the empirical measurements, the shape of the response is very similar, and the frequency of oscillation is relatively well matched.

In Fig. 10 appears the response of the mass flow rate control system to the same 50 SLM step command input as in Fig. 9, but with the control law implemented as designed. The oscillations have been eliminated and the speed of response is as quick as the hardware allows. The control voltage input to the valve actuator is plotted vs time along with the measured mass flow rate vs time to demonstrate that although the mass flow meter shows a lag in response, the control voltage reaches zero very quickly. At this point, the valve has reached steady-state meaning that the mass flow rate has been set constant within about 6 s, while the lagged response of the meter cannot verify this for as long as 25 s. The theoretical simulation data appear with the empirical data and show excellent agreement.

The next set of data demonstrates the operation of the mass flow rate controller under different upstream pressure conditions. In Figs. 9 and 10, the upstream pressure was set to 1000 psig, while in this case (Fig. 11) the upstream pressure has been reduced to 625 psig. Additionally, the nitrogen was allowed to flow until the pressure had equalized between the source and fill tanks to help determine the limit of the controller's ability to maintain a mass flow rate under these conditions. The plots show that the control system is operating very well under these lower pressure conditions, and that the mass flow rate is kept to within 1% of the command value until the fill tank pressure reaches about 85% of the upstream pressure. In this case, the valve orifice unchokes at about 71 s, yet the mass flow rate is maintained roughly constant for another 45 s, which is a significant improvement over the sonic orifice method of setting mass flow rates.

Mass Ratio Controller

Measurements of the mass ratio control system have been made in order to demonstrate that the control law is operating as designed. Independent measurements of the accumulating mass have also been made during these runs in order to determine the accuracy limitations in the mass ratio control system.

The error in the final mass ratio to be set by this control system depends upon two factors: 1) the integral error of the mass flow meter reading and 2) the error introduced in the control loop due to discrete integration. With these factors

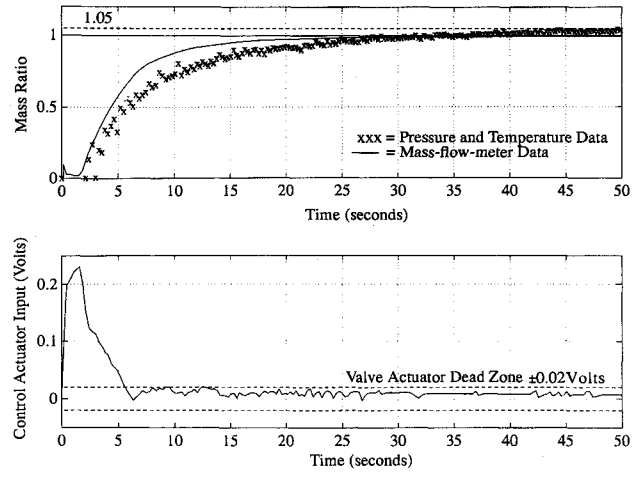

Fig. 12 Mass ratio controller operating with nitrogen gas at an upstream pressure of 1000 psig demonstrates that the control law operates properly. The plot of control actuator input shows that the valve has been set to its steady-state value in under 6 s.

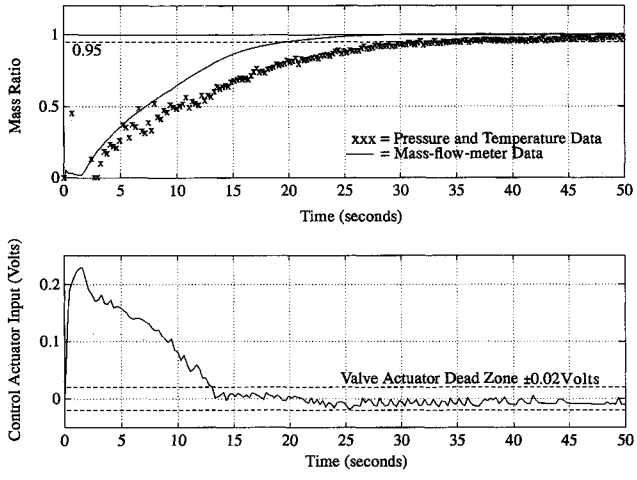

Fig. 13 Mass ratio controller operating with nitrogen gas at an upstream pressure of 600 psig demonstrates that the control law can still maintain an accurate mass ratio setting under different pressure conditions. The plot of control actuator input vs time shows that the valve has reached steady state within about 12.5 s.

accounted for, the percent error in the final mass ratio is given by

$$E_{MR} = \frac{2E_p}{(1 - E_p)} \tag{37}$$

where the percent error in the mass flow meter measurement E_p has been assumed to be equal in magnitude for the computation of the command mass error and the feedback mass error. This relationship shows that the error in the mass ratio is about twice that of the error in the mass flow rate measurement, so that the mass flow meters must be calibrated to twice the accuracy that the final mass ratio is desired to have.

Since the prototype system consists of only one valve and meter, the command signal to the mass ratio control system must be simulated. This is accomplished by applying a step command input with the computer software that simulates the case where the primary gas is already flowing at a constant rate when the mass ratio control system is turned on. All runs use nitrogen gas and the system is set up to achieve mass ratios equal to unity for simplicity in the data reduction.

The first set of data (Fig. 12) has been recorded with an upstream gas pressure of 1000 psig and a simulated command input of 50 SLM. The plot of mass ratio vs time shows both the data from within the control loop and that from the pressure and temperature calculations of the accumulated mass. The control loop data demonstrated that the control law is operating properly by setting the mass ratio to the command value of unity. A discrepancy of about 5% between the two independent measurements arises from the error in the pressure and temperature measurements and whatever error exists in the mass flow meter calibration. The narrowing of the accuracy limits for the mass ratio controller may require a more accurate calibration, but the independent measurements are within the experimental error of the measurement probes, so that the concept of mass ratio control has been validated.

The second set of data (Fig. 13) shows the operation of the mass ratio controller under lower pressure conditions for the same simulated command input of 50 SLM. The control system appears to be very effective in this case and the pressure and temperature data are in better agreement than before. Whether or not this is an effect due to the varying pressure cannot be verified without employing measurement probes with higher accuracy.

Conclusions

The concept of setting mass ratios with a feedback controller employing RTD mass flow meters and switched servoactuated valves has been validated. The operation of both the mass flow rate and the mass ratio control subsystems has been verified through independent measurements of accumulated mass to work within experimental accuracy. Furthermore, the analysis in this article has shown that the accuracy of this type of feedback-controlled gas mixing system is dependent only upon the calibration accuracy of the mass flow meters that are employed. Subsequent analysis at the University of Washington[6] has demonstrated that this type of control will also work with CO_2, which exhibits nonideal behavior.

Acknowledgments

This work was supported in part by U.S. Air Force Contract F08635-89-C-0196. The authors wish to express their gratitude to the following for their research efforts in support of this work: J. Auzias de Turenne, E. Burnham, G. Chew, B. Dunmire, A. Higgins, J. Hinkey, and C. Knowlen. The authors also wish to thank A. Hertzberg and T. Mattick for their contributions and discussions, and D. Bogdanoff for the information and consultations he provided regarding current research in shock-tunnel gas mixing systems at NASA Ames Research Center. Finally, the equipment and expertise in control systems supplied by J. Vagners has greatly enhanced the quality of research presented here.

References

[1]Hertzberg, A., Bruckner, A. P., and Bogdanoff, D. W., "Ram Accelerator: A New Chemical Method for Accelerating Projectiles to Ultrahigh Velocities," *AIAA Journal*, Vol. 26, No. 2, 1988, pp. 195–203.

[2]Higgins, A. J., Knowlen, C., and Bruckner, A. P., "An Investigation of Ram Accelerator Gas Dynamic Limits," AIAA Paper 93-2181, June 1993.

[3]Olin, et al., U.S. Patent 4,487,062, Dec. 11, 1984.

[4]Lyons, J. L., *Lyons' Valve Designers Handbook*, Reinhold, New York, 1982, pp. 180–185.

[5]Shames, I. H., *Mechanics of Fluids*, McGraw-Hill, New York, 1962, Sec. 11.19.

[6]Koch, A., "Analysis of a Gas Mixing System Flowing a Non-Ideal Test Gas," AIAA 43rd Region VI Student Conference, Tucson, AZ, April 1993.